Available online at www.sciencedirect.com
ScienceDirect
Journal of Inorganic Biochemistry 102 (2008) 1473–1485
Journal of Inorganic Biochemistry
www.elsevier.com/locate/jinorgbio

Interactions of insulin–mimetic zinc(II) complexes with cell constituents: Glutathione and ATP

Éva Anna Enyedy [a], Andrea Lakatos [a], László Horváth [a], Tamás Kiss [a,b,*]

[a] Department of Inorganic and Analytical Chemistry, University of Szeged, P.O. Box 440, H-6701 Szeged, Hungary
[b] Bioinorganic Chemistry Research Group of the Hungarian Academy of Sciences, P.O. Box 440, H-6701 Szeged, Hungary

Received 8 August 2007; received in revised form 4 January 2008; accepted 4 January 2008
Available online 16 January 2008

Abstract

Ternary complex formation of some potent insulin–mimetic zinc(II) complexes of bidentate ligands: maltol and 3-hydroxy-1,2-dimethyl-pyridinone with (O,O), 2-picolinic acid and 6-methylpicolinic acid with (N,O) and the tridentate 2,6-dipicolinic acid with (O,N,O) coordination modes was studied in aqueous solutions by pH-potentiometry and spectroscopic (UV, CD, ESI-MS) methods in the presence of critical cell constituents such as L-glutathione reduced (GSH) and adenosine 5′-triphosphate (ATP). Results showed that formation of the ternary complexes was hindered in the case of 2,6-dipicolinic acid, especially with ATP, while it was favoured with the bidentate ligands in the physiological pH range. Driving force of the formation of mixed-ligand species was found to be a more enhanced coordination of GSH and ATP as second ligands in the ternary complexes than in their binary ones due to steric and electrostatic reasons. The mitochondrial dehydrogenase activity of the zinc(II) complexes, as an indirect indicator for the glucose intake, was measured on Mono Mac and 3T3-L1 adipocyte cell lines. The activity of the complexes up to ~10–100 μM concentration was in the range of the effect of 0.75–1.5 μM insulin, while at higher concentration it was broken down due to the sensitivity of the cells to toxicity of the complexes.

Keywords: Insulin–mimetic zinc(II) complexes; Solution equilibrium study; Ternary complexes; Glutathione; ATP

1. Introduction

After the first confirmation of the insulin–mimetic effect of zinc-chloride in rat diabetes models [1], in the last few years more and more antidiabetic zinc(II) complexes were developed and studied both *in vitro* and *in vivo*. The efficiency and the absorption of the metal ion can be enhanced by complex formation, since the potent ligands such as maltol (mal), 6-methylpicolinic acid (6-Me-pic), allixin, *N*-methylthioallixin or different dithiocarboxylic acids etc., form neutral, small sized bis complexes with reasonably high lipophylic character [2–6]. Hopefully, zinc(II) complexes can be better hypoglycaemic drug candidates than vanadium ones, due to the low toxicity and higher bioavailability of this essential metal ion. However, it is important to note that the efficiency of zinc(II) complexes is lower than that of oxovanadium(IV) complexes [7].

The effect of the zinc(II) complexes studied on glucose uptake into the cells is fairly complicated and the mechanism is not completely revealed yet. *In vitro* studies performed on rat adipocytes showed that the insulin–mimetic complexes act at different sites of insulin signalling, they activate tyrosine kinase of the insulin receptor, phosphatidyl inositol-3 kinase, phosphodiesterase enzymes and glucose transporters, and they may inhibit the protein tyrosine phosphatase [8]. Moreover, there is no information about the actual chemical form of the zinc(II) complex after entering the cell. Most probably the original form does not

* Corresponding author. Address: Department of Inorganic and Analytical Chemistry, University of Szeged, P.O. Box 440, H-6701 Szeged, Hungary. Tel.: +36 62 544337; fax: +36 62 420505.
E-mail address: tkiss@chem.u-szeged.hu (T. Kiss).

0162-0134/$ - see front matter © 2008 Elsevier Inc. All rights reserved.
doi:10.1016/j.jinorgbio.2008.01.007

remain as the complex can interact with endogenous zinc(II) binders such as L-glutathione reduced (γ-L-glutamyl-L-cysteinyl-glycine, GSH) and oxidised (GSSG) or adenosine 5′-triphosphate (ATP) which can be found in high concentrations in the cytosol (0.5–20 mM and 2–4 mM, respectively) [9,10]. The GSH/GSSG pair is involved in the cellular mobilization and transport processes of zinc(II) [11–13]. ATP is the main biomolecule responsible for the energy transfer, hence it is one of the most important metabolic substances. Its active form is usually a complex with magnesium(II), however, as zinc(II) forms somewhat stronger complexes with ATP [14], zinc(II) may also participate in the enzymatic processes of ATP production [15]. *In vitro* studies on the ternary complex formation between potent insulin–mimetic compounds and relevant critical cell constituents may provide useful information to a better understanding of their action. In the case of insulin–mimetic vanadium complexes of mal ternary complex formation with GSH and ATP could be detected only at high excess of these two biomolecules and GSH was found mostly to participate in the reduction of V(V)–V(IV), while ATP to complex VO(IV) in various binary and ternary complexes [10]. Although, ATP is continuously hydrolysed to and then reformed from adenosine diphosphate (ADP) or adenosine monophosphate (AMP), these metal ions form complexes with them with one or two and a half magnitude lower stability, respectively than ATP [14] does. Hence, ADP and AMP can not be regarded as efficient competitors of ATP in these complexation reactions. Moreover, ATP contains a terminal primary oligophosphate group, which has strong metal binding ability. Accordingly, it can serve as a model compound for other metal binder nucleotides and organophosphates.

In this paper complex formation equilibria of mixed-ligand complexes between zinc(II), mal, 3-hydroxy-1,2-dimethyl-pyridinone (dhp), 2-picolinic acid (pic), 6-Me-pic, 2,6-dipicolinic acid (dipic), as ligands A and GSH, ATP as ligands B, were studied by pH-potentiometry, UV spectrophotometry, circular dichroism (CD) spectroscopy and electrospray ionization mass spectrometry (ESI-MS). The bis complexes of ligands A with the exception of dipic were tested already in the literature by either *in vitro* or *in vivo* studies and proved to be biologically active [3,5,16–18]. Therefore, in the present work, *in vitro* biological studies were performed with the bis dipicolinato-zinc(II) complex too, and of $[Zn(mal)_2]$ and $[Zn(pic)_2]$ for comparison on human Mono Mac and 3T3-L1 adipocyte cells in order to obtain information about their insulin–mimetic efficiency and cell toxicity.

2. Experimental

2.1. Chemicals

All ligands except dhp were commercially available products of *puriss* quality (Aldrich, Sigma or Fluka), while dhp was prepared as described earlier [19]. Their purities were checked and the exact concentrations of the prepared stock solutions were determined by the Gran method [20]. A $ZnCl_2$ stock solution was made by the solution of anhydrous $ZnCl_2$ in known amount of HCl and its concentration was determined by complexometry via the EDTA complex and by gravimetrically via the oxinate.

2.2. pH-potentiometric studies

The pH-metric measurements for determining stability constants of the proton and zinc(II) complexes of the ligands were carried out at an ionic strength of 0.2 M KCl and at 25.0 ± 0.1 °C. The titrations were performed with a carbonate-free KOH solution of known concentrations (*ca.* 0.2 M). An Orion 710A pH-meter equipped with Metrohm combined electrode (type 6.0234.100) and Metrohm 665 Dosimat burette were used for the pH-metric measurements. The electrode system was calibrated according to Irving et al. [21] and therefore the pH-meter readings could be converted into hydrogen ion concentration. The water ionization constant, pK_w, is 13.76 ± 0.01 under the conditions employed. The pH-metric titrations were performed in the pH range 2.0–11.0, or until precipitation occurred in the samples. Initial volume of the samples was 10.00 mL. The ligand concentrations varied in the range 2×10^{-3}–4×10^{-3} M. In the binary systems the metal ion to ligand ratios were 1:1, 1:2 and 1:4 and in the ternary systems metal:ligand A:ligand B 1:1:1, 1:2:1, 1:1:2, 1:2:2. The accepted fitting of the titration curves always was less than 0.01 mL and the uncertainties (3SD values, which mean the triple values of the standard deviations) in the stability constants are given in parentheses in the Tables. The samples were in all cases completely deoxygenated by bubbling purified argon for *ca.* 15 min before the measurements and argon was also passed across the solutions during the titrations. Duplicate titrations were carried out and the reproducibility of titration points included in the evaluation was within 0.005 pH unit throughout the pH range. pH-potentiometric results were utilised to establish the stoichiometry of species and to calculate the stability constants ($\log\beta$). Calculations were always made from the experimental titration data received before the precipitation with the computer program PSEQUAD [22].

2.3. Spectroscopic measurements

UV spectrophotometric measurements on systems containing dipic in 1.6×10^{-4} M, GSH and mal in 8.0×10^{-5} M concentrations were performed, and the zinc(II) to dipic ratios were 0:1, 1:2 and zinc(II) to mal to GSH ratios were 0:1:0, 1:2:0, 0:0:1, 1:0:2, 1:2:2 in the pH range from 2 to 11. An Unicam Helios Alpha spectrophotometer was used to record the spectra in the region of 205–450 nm. Path length was 1 cm. Protonation and stability constants, and the individual spectra of the species were calculated by the computer program PSEQUAD [22].

CD spectra were recorded on a Jobin-Yvon Mark VI dichrograph in the wavelength interval from 210 to 350 nm, in an optical cell of 0.20 cm path length (l) at 25 °C. The analytical concentration of GSH was 8.0×10^{-4} M and zinc(II) to mal to GSH ratios were 0:0:1, 1:0:2, 1:2:2 and pH was varied between 2 and 11. CD data are given as the differences in molar absorptivities between left and right circularly polarized light, based on the concentration of GSH ($\Delta\varepsilon = \Delta A/l/c_{GSH}$).

Due to the oxygen sensitivity of GSH the samples were always completely deoxygenated by bubbling nitrogen through them before the spectroscopic measurements.

2.4. ESI-MS measurements

ESI-MS spectra were recorded on an LCQ Deca (ThermoFinnigan, San Jose, CA, USA) ion trap instrument working in positive ion mode. Samples were introduced into the ESI source by direct infusion via a syringe pump at a flow rate of 5 μL/min. The capillary temperature as maintained at 180 °C, the spray voltage was fixed at 4 kV and the sheat gas flow rate was 40 (a.u). These parameters gave a stable spray during measurements. MS^n experiments on preselected ion species were performed by application of supplementary rf voltage in the range of 0–5 V with helium as target gas. The solvent used for sample preparation was a water/acetonitrile (ACN) 1:1 mixture prepared from MilliQ grade water and HPLC grade ACN. The concentrations employed were 20 μM and 40 μM for the metal ion and the zinc(II):A:GSH ratios were 1:2:1, 1:2:2 and in some cases 1:2:3 and 1:2:4. Measurements were carried out at pH 7. The pH of the solutions were measured with a Metrohm 6.0234.100 combined glass electrode, previously calibrated in pH 4.01 and pH 7.00 aqueous standard buffer solutions. No corrections were made for the presence of ACN. The pH of the sample solutions were set to the desired values by addition of 0.1 M aqueous NH_3 and HCl (Fluka products).

2.5. Cell cultures and biological tests

Tests were performed on a Mono Mac human monocyte and a 3T3-L1 adipocyte cell culture. The cells were maintained in GIBCO® Advanced RPMI tissue culture medium or in DMEM in the case of 3T3-L1 adipocyte cells, supplemented with 0.63 mg/ml-glutamine, 10NE units of penicillin (TEVA-Biogal, Hungary) and 0.1 mg/ml of streptomycin (EGISZ, Hungary) and 5% or 10% (with 3T3-L1 cells) fetal calf serum (FCS) (GIBCO) at 37 °C under a humidified atmosphere containing 5% CO_2.

In all tests, an insulin group (cells incubated with insulin instead of the zinc(II) compound) and a control group (neither insulin nor zinc(II) compound present) were included, and all tests were carried out with three parallels. The carrier ligands (mal, pic and dipic) were dissolved in a stock solution of zinc(II) chloride (metal to ligand ratio was 1:2; $c_{zinc(II)}$ was 0.01 M), $NaHCO_3$, NaCl, KCl (in a concentration of 0.024 M, 0.137 M, 0.0027 M, respectively)) followed by sterile filtration. The biological effects of the ligands alone were tested before [23,24] and were found to be negligible. The inorganic salts of zinc(II) are biologically active, e.g. the IC_{50} value of $ZnSO_4$ is 0.81 ± 0.10 mM, while for the zinc(II) complexes of mal and pic is 0.59 ± 0.10 mM and 0.64 ± 0.13 mM, respectively [2,3,18].

For toxicity tests, Mono Mac cells (10^5 cells/well) were grown in RPMI, 5% FCS in 96 multi-well plates in the presence or absence of the zinc(II) complexes for 48 h. The cells were spinned with 1600 rpm for 5 min. The supernatant medium was discarded and the cells were washed with phosphate buffered saline solution (PBS), then resuspended in 300 μL of PBS containing 10 μg/ml propidium iodide (PI). Cells which become PI(positive) were considered as dead cells and analyzed by cytofluorimetry (FACSCalibur Beckton and Dickinson) using an excitation wavelength of 485 nm and an emission wavelength of 650 nm. Results are expressed as the percent increase in the red fluorescence of treated cells over the fluorescence of control cells (no treatments), i.e., $100 \times (PI_{treatment} - PI_{control})/PI_{control}$).

Tests for insulin–mimetic activity were based on the EZ4U® (Biomedica) cell proliferation and cytotoxic assay. The method is based on the finding that living cells, absorbing glucose, are capable to reduce slightly yellow or uncoloured tetrazolium salts into intensely coloured red formazan derivatives. The reduction requiring functional mitochondria which are inactivated within few minutes after cell death. In this assay, 200 μL of cultured cells were incubated in the presence or absence of the zinc(II) complexes or insulin for 48 h, then 20 μL of EZ4U was added for the required time (1.5–3 h). Formazan production, which was linearly related to cell number, was assayed by measuring optical density (OD) at 492 nm wavelength in an ELISA microplate autoreader. The EZ4U test measures only the metabolic activity of mitochondria, which may not be connected directly with the activity of glucose uptake. This method was used only as a primary assay for screening the Zn(II) compounds, although we have demonstrated the validity of this test by comparing the test results with those based on the uptake of tritiated glucose [7]. The real effectiveness of the best compounds for actual glucose uptake will be tested by [^{3}H] glucose.

3. Results and discussion

3.1. Binary complexes

3.1.1. Binary complexes of the carrier ligands

Formulae of the ligands studied in their fully protonated forms can be found in Scheme 1 and their protonation constants with the stoichiometries and stability constants of complexes formed with zinc(II) are collected in Table 1.

Complexation processes of mal, dhp, pic and 6-Me-pic with zinc(II) have already been studied in our laboratory

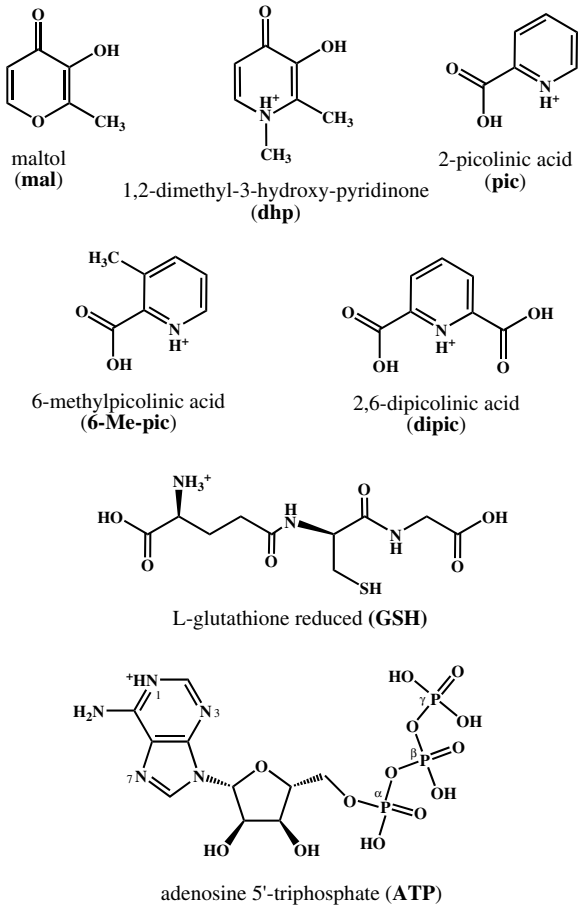

Scheme 1. Formulae of the ligands studied in their fully protonated forms.

[5], but all constants were redetermined and showed good agreement with the literature data measured under identical conditions within the experimental error. These bidentate ligands form $[ZnA]^{+}$, $[ZnA_2]$, $[ZnA_3]^{-}$, $[ZnA_2H_{-1}]^{-}$ complexes, however, coordination of the third ligand in the order of pic, 6-Me-pic, mal, dhp becomes less and less favoured and mixed hydroxo species were detected in the basic pH range. Mal and dhp coordinate to zinc(II) via oxygen donors while in the complexes of pic and 6-Me-pic the pyridine-nitrogen and the carboxylate-oxygen are coordinated [5].

Protonation constants of dipic were redetermined in the present work and the dissociation processes were also followed by UV spectrophotometric measurements. The calculated values are similar to those reported in the literature [25] and are in good agreement with the potentiometric data (see Table 1).

Stability constants for zinc(II) complexes of dipic were not available under our experimental conditions; data determined in the present work are listed in Table 1. The concentration distribution curves depicted in Fig. 1 reveal that $[ZnA_2]^{2-}$ is the predominant complex almost in the whole pH range studied. Considering the very low value of $\log K(ZnA)/\log K(ZnA_2)$, binding of the second dipic to [ZnA] is significantly favoured. In this bis complex, in contrast with the other insulin–mimetic bis complexes, most probably all the coordination sites are occupied by the tridentate (O,N,O) coordination of two dipic ligands. Tridentate coordination mode was proved by X-ray structure in the case of $[ZnA_2H_2]$ complex [26] and the coordination of the carboxylates by IR for $Na_2[ZnA_2]$ [27]. UV spectra were recorded also for the zinc(II)–dipic system and stability constants calculated from the spectra are collected in Table 1, these values correspond well to the data obtained by pH-potentiometry. Individual spectra calculated for some zinc(II) complexes of dipic show much better resolved fine structures than in case of the free dipic ligand. (ε $[ZnA] = 5.1 \times 10^3\ M^{-1}\ cm^{-1}$ (268 nm); $\varepsilon\ [ZnA_2]^{2-} = 1.11 \times 10^4\ M^{-1}\ cm^{-1}$(269 nm); $\varepsilon\ [ZnAH_{-1}]^{-} = 5.9 \times 10^3\ M^{-1}\ cm^{-1}$ (270 nm)).

Conditional stability constants of the bis insulin–mimetic complexes at physiological pH are shown in the last row of Table 1, since the stability of these complexes is more easily comparable at a given pH by these constants. The stability order reveals that in accordance with the expectation, introduction of a second carboxylate at a chelatable position to the pic increased the stability significantly in the case of dipic in contrast with the 6-methyl group.

3.1.2. Binary complexes of GSH

Protonation constants of GSH, as well as stability constants of zinc(II) complexes are listed in Table 1; the speciation model was the same as published earlier under different conditions [28,29]. $\log K(HB)$ and $\log K(H_2B)$ belong mostly to the overlapping protonation of the thiolate and amine groups and the two lower constants to the protonation of the carboxylates. Since zinc(II) is a borderline metal ion and GSH has eight possible donor atoms a wide variety of coordination modes may be assumed in the zinc(II) complexes of GSH. The generally accepted view is that the thiolate sulphur is always involved in the coordination together with the terminal Gly residue at lower pH and with the side chain carboxylate of Glu with increasing pH [30]. Zinc(II) induced amide deprotonation was suggested above pH 10.5 on the basis of ^1H and ^{13}C NMR measurements, most probably in species $[ZnB_2H_{-2}]^{6-}$ [31]. At physiological pH $[ZnB_2H]^{3-}$ is the predominant species, in which one GSH is coordinated in a tridentate way via (S^-, COO^- (Glu), NH_2(Glu)) donor set and the other through a monodentate thiolate in its proposed structure [29].

UV and CD spectra were recorded on GSH and zinc(II)–GSH system as a function of pH. Titrations of GSH showed a considerable enhancement in absorbances above pH 8 where overlapping deprotonation of $[H_2B]^{-}$ and $[HB]^{2-}$ takes place, consequently higher molar absorptivities could be determined based on the macroscopic constants for $[HB]^{2-}$ and mainly for $[B]^{3-}$ compared with the other protonated species of GSH as individual spectra show in Fig. 2.

Table 1
Protonation constants ($\log K$) of the ligands studied and stability constants ($\log \beta$) of their Zn(II) complexes with some stepwise and conditional stability constants at $t = 25$ °C; $I = 0.20$ M KCl[a]

	mal[b]	dhp[b]	pic[b]	6-Me-pic[b]	dipic[c]	dipic[d]	GSH[e]	ATP[f]
$\log K$ (HA)	8.44	9.77	5.19	5.81	4.58(0.01)	4.61(0.02)	9.48(0.01)	6.36(0.01)
$\log K$ (H_2A)		3.67	~1	~1.2	2.08(0.02)	–	8.63(0.01)	3.96(0.02)
$\log K$ (H_3A)	–	–	–	–	~1.0	–	3.43(0.02)	~1.5
$\log K$ (H_4A)	–	–	–	–	–	–	2.11(0.02)	
$\log \beta$ (ZnAH)							14.48(0.03)	8.84(0.08)
$\log \beta$ (ZnA)	5.57	7.24	5.19	4.02	6.25(0.11)	6.49(0.05)	8.03(0.01)	4.69(0.03)
$\log \beta$ ($ZnAH_{-1}$)	–	–	–	–	−1.55(0.10)	−1.66(0.04)	–	−3.98(0.05)
$\log \beta$ ($ZnAH_{-2}$)	–	–	–	–	–	–	–	−13.83(0.15)
$\log \beta$ (ZnA_2H_2)	–	–	–	–	–	–	28.76(0.03)	–
$\log \beta$ (ZnA_2H)	–	–	–	–	13.85(0.21)	–	21.84(0.02)	–
$\log \beta$ (ZnA_2)	10.29	13.55	9.52	7.98	12.77(0.08)	12.84(0.07)	12.80(0.03)	7.21(0.16)
$\log \beta$ (ZnA_2H_{-1})	−0.1	2.3	0.7	−1.7	1.15(0.21)	–	2.54(0.20)	–
$\log \beta$ (ZnA_2H_{-2})	–	–	–	–	–	–	−7.42(0.21)	–
$\log \beta$ (ZnA_3)	12.71	15.2	13.07	10.30	–	–	–	–
$\log K$ (ZnA)	5.57	7.24	5.19	4.02	6.25	6.49	8.03	4.69
$\log K$ (ZnA_2)	4.72	6.31	4.33	3.96	6.52	6.35	4.77	2.52
$\log K$ (ZnA_3)	2.42	1.65	3.55	2.32	–	–	–	–
$\log(K(ZnA)/K(ZnA_2))$	0.85	0.93	0.86	0.06	−0.27	0.14	3.26	2.17
$\log(K(ZnA_2)/K(ZnA_3))$	2.30	4.66	0.78	1.64	–	–	–	–
$\log \beta^*(ZnA_2)$[g]	8.13	8.86	9.52	7.96	12.77	–	–	–

[a] Standard deviations (3 × SD) in parenthesis are shown if the values were determined in the present work. "A" generally marks the completely deprotonated form of the ligands in this table.
[b] Ref. [5].
[c] Fitting parameter: 7.15×10^{-3} mL, number of points: 460, pH range: 2–10.
[d] Determined by UV spectrophotometry, fitting factor: 6.45×10^{-3}.
[e] Fitting parameter: 1.47×10^{-3} mL, number of points: 399, pH range: 2–10.
[f] Fitting parameter: 5.48×10^{-3} mL, number of points: 325, pH range: 2–10.
[g] Conditional stability constants at pH 7.4; $\log \beta^*(ZnA_2) = \log \beta\ (ZnA_2)/(\alpha_H)^2$; $\alpha_H = 1 + \sum_i \beta_{H_iA}[H^+]^i$.

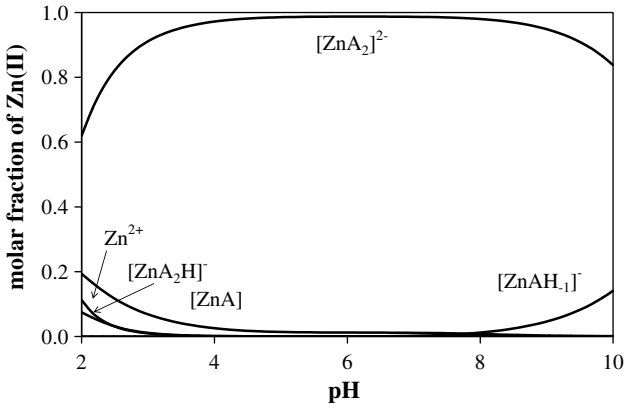

Fig. 1. Concentration distribution curves for complexes formed in the Zn(II)–dipic system at 1:2: metal ion to ligand ratio, $c_{Zn(II)} = 2$ mM.

CD spectra of GSH represent the development of a characteristic band with positive Cotton-effect above pH 8. ($\Delta\varepsilon$ $[H_2B] = -1.875$ $M^{-1}\,cm^{-1}$ (210 nm); $\Delta\varepsilon$ $[B]^{3-} = +3.250$ $M^{-1}\,cm^{-1}$ (210 nm)). Changes in the UV and CD spectra of the ligand were similar in the case of addition of zinc(II) to GSH, but they started at lower pH parallel to the formation of metal complexes. Differences between absorbances of zinc(II)–GSH system and those of GSH alone detected by UV measurements at the same pH values are shown in the inset of Fig. 2. The increase in UV absorbance (i.e., at 220 nm) in the presence of zinc(II) above pH 7 is considered tentatively as the development of a metal to ligand charge transfer (MLCT) band in the literature [32]. No doubt about the coordination of thiolate sulphur to zinc(II) in the metal complexes of GSH [33], but our results show that changes in the spectra correspond merely to the metal induced deprotonation of the ligand and not necessarily to a MLCT band. Additional changes could be observed by comparison of the UV and CD spectra of zinc(II)–GSH system with those of GSH alone above pH 9. Namely, absorbances in the UV spectra started to decrease considerably in the range of 235–260 nm as inset of Fig. 2 at 250 nm shows. Moreover, an intensive broad band with negative Cotton-effect developed in the CD spectra due to the formation of $[ZnB_2H_{-2}]^{6-}$ complex. ($\Delta\varepsilon$ $[ZnB_2H_{-2}]^{6-} = -8.750$ $M^{-1}cm^{-1}$ (222 nm)). As a conclusion, nothing more can be clearly stated from the spectroscopic measurements than the zinc(II) induced amide coordination seems to result in significant changes in the electron structure and the conformation of the GSH molecule.

3.1.3. Binary complexes of ATP

Protonation constants of ATP listed in Table 1 were determined in a solution containing 4 mM of ligand and under this condition the self-association processes are almost completely negligible [34]. Calculations revealed constants in good agreement with literature data [35,36].

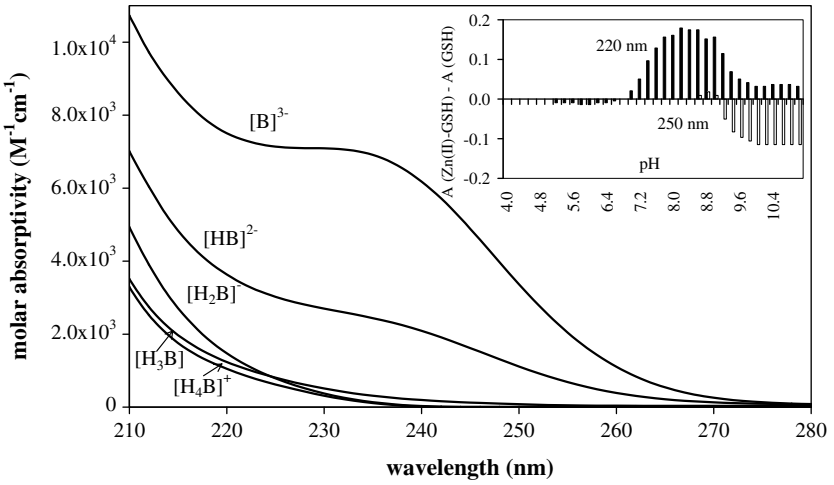

Fig. 2. Individual UV spectra of GSH species. Inset shows differences between absorbances of Zn(II)–GSH system and those of GSH plotted against pH at 220 nm (black bars) and at 250 nm (stripe bars), $c_{GSH} = 8.0 \times 10^{-5}$ M, metal to ligand ratio is 1:2.

ATP protonates first at the γ-phosphate group, then in a slightly overlapping process N-1 nitrogen picks up a proton. An extra protonation constant due to a phosphate group could be determined with lower accuracy in the acidic region. ATP is a molecule which can bind metal ions at three potential binding sites such as the phosphate donor groups, the ring nitrogen (N-7) of adenine moiety or the sugar hydroxo groups. In the case of zinc(II) several mono complexes with different protonation levels could be detected with the formation of $[ZnB_2]^{6-}$ bis complex in the studied pH range. An isomeric equilibrium due to the two possible protonation sites (N-1 and γ-phosphate group) in $[ZnBH]^-$ complex with relevant intramolecular equilibria have been already considered in details in the literature [35]. Sigel and co-workers also showed that besides the predominant binding of phosphate oxygens to zinc(II), the participation of N-7 adenine residue in the coordination resulting in the formation of inner and outer sphere macrochelates is also significant in the complex $[ZnB]^{2-}$ [35]. At higher pH values most probably formation of mixed-hydroxo species ($[ZnBH_{-1}]^{3-}$ and $[ZnBH_{-2}]^{4-}$) takes place. In addition, the relatively high positive value of $\log K(ZnB) - \log K(ZnB_2)$ shows an unfavourable coordination of a second ATP molecule to the $[ZnB]^{2-}$ core. In the bis complex most probably the phosphate donors bind to zinc(II).

3.2. Ternary complexes

None of the ligands studied is able to saturate the coordination sphere of zinc(II) by the binding of only a single molecule what makes formation of the ternary complexes possible. Accordingly, mixed-ligand complexes with various compositions were detected in the zinc(II)–carrier ligand (mal, dhp, pic, 6-Me-pic, dipic)–GSH and zinc(II)–carrier ligand–ATP systems. The equilibrium models together with the calculated stability constants are collected in Table 2.

As Table 2 shows 1:1:1 and 1:2:1 zinc(II):carrier ligand:GSH (or ATP) complexes are formed in almost all systems, however, no *tris* ternary complexes could be determined for the tridentate dipic in accordance with the expectations. However, in the case of ATP the formation of [ZnABH] complexes could be calculated only with high inaccuracy. It is also important to note that no ternary complex formation was found in the zinc(II)–dipic–ATP system under our conditions. A comparison of the stepwise equilibrium constants for the deprotonation processes of the ternary complexes listed in Table 3 with those of the parent complexes and protonation constants of the free ligands, it can be concluded that assuming monodentate thiolate coordination of GSH as in the binary bis complex $[ZnB_2H]$, the proton can be assigned most probably to the amino group of GSH in the ternary complexes [ZnABH] and $[ZnA_2BH]$. The pK(ZnABH) and pK (ZnA_2BH) values are much lower than the first protonation constant of GSH. Accordingly, these deprotonations are probably accompanied by a structural rearrangement to (S^-,NH_2(Glu)) coordination mode of GSH in complexes [ZnAB] and $[ZnA_2B]$. The coordination of thiolate sulphur accompanied by the binding of the terminal amino nitrogen in the ternary complexes, as shown in Scheme 2, was confirmed by ESI-MS measurements (see Section 3.3). Literature data suggest pentacoordinate zinc(II) in these complexes [37,38]. Due to the high pK(ZnA_2BH) value in the case of dhp, its $[ZnA_2B]$ complex seems to be an exception, a mixed hydroxo species with protonated amino group of GSH is suggested and $[ZnA_2BH(OH)]$ is the more probable formula. According to the limitation of pH-potentiometry we can not distinguish between the two binding modes, but formation of the latter species in the basic pH range, where mixed hydroxo species are predominant in the binary system, confirms this assumption. Deprotonation of a coordinated water molecule in [ZnAB] complexes of both GSH and ATP ligands occurs with pK ~10.

Table 2
Models and overall stability constants ($\log\beta$) for the mixed-ligand complexes formed in the Zn(II) – carrier ligand (A)–GSH (B)/ATP (B) ternary systems ($t = 25$ °C; $I = 0.20$ M KCl)

	mal	dhp	pic	6-Me-pic	dipic
B = GSH					
[ZnABH]	19.57(0.08)	21.50(0.07)	19.31(0.17)	18.45(0.29)	21.24(0.14)
[ZnAB]	12.11(0.05)	13.34(0.15)	11.94(0.16)	11.63(0.08)	13.24(0.08)
[ZnABH$_{-1}$]	2.05(0.07)	2.92(0.18)	2.40(0.08)	1.79(0.12)	–
[ZnA$_2$BH]	23.74(0.05)	26.70(0.08)	22.79(0.36)	22.31(0.08)	–
[ZnA$_2$B]	–	16.77(0.14)	14.98(0.15)	–	–
Fitting (mL)	2.94×10^{-3}	4.35×10^{-3}	4.92×10^{-3}	6.08×10^{-3}	7.15×10^{-3}
No. of points	582	617	532	572	460
pH range	2–10	2–10.8	2–10	2–10	2–10.7
B = ATP					
[ZnAB]	9.31(0.03)	11.15(0.03)	9.41(0.06)	8.14(0.03)	–
[ZnABH$_{-1}$]	−0.62(0.09)	1.15(0.11)	–	–	–
[ZnA$_2$B]	–	15.35(0.22)	–	–	–
Fitting (mL)	2.25×10^{-3}	3.13×10^{-3}	7.18×10^{-3}	2.05×10^{-3}	–
No. of points	421	467	295	322	379
pH range	2–9	2–10.5	2–9	2–8	2–10

Table 3
Some stepwise, conditional and derived stability constants for the mixed-ligand complexes formed in the Zn(II) – carrier ligand (A)–GSH (B)/ATP (B) systems and summed molar fractions calculated for the ternary complexes and parent complexes of carrier ligands formed at pH 7.40

	mal	dhp	pic	6-Me-pic	dipic
B = GSH					
pK (ZnABH)	7.46	8.16	7.37	6.82	8.00
pK (ZnAB)	10.06	10.42	9.54	9.84	–
pK (ZnA$_2$BH)	–	9.93	7.81	–	–
$\log K$ (ZnA + BH)[a]	14.00	14.26	14.12	14.43	14.99
$\log K$ (ZnA$_2$ + BH)[a]	13.45	13.15	13.27	14.33	–
$\log K$ (ZnA + B)[b]	6.54	6.10	6.75	7.61	6.99
$\log K$ (ZnB + A)[c]	4.08	5.31	3.91	3.60	5.21
$\log\beta^*$ (ZnABH)[d]	17.24	17.90	18.05	17.18	19.98
$\log\beta^*$ (ZnAB)[d]	7.70	7.66	8.60	8.28	9.90
$\log\beta^*$ (ZnA$_2$BH)[d]	20.33	20.76	21.53	21.03	–
Σ[Zn−A−B][e]	0.47	0.57	0.36	0.73	0.11
Σ[Zn−A][e]	0.25	0.25	0.46	0.07	0.88
B = ATP					
pK (ZnAB)	9.93	10.00	–	–	–
$\log K$ (ZnA + B)[f]	3.74	3.91	4.22	4.12	–
$\log K$ (ZnB + A)[c]	4.62	6.46	4.72	3.45	–
$\log\beta^*$ (ZnAB)[d]	8.19	8.77	9.37	8.09	–
Σ[Zn–A–B][e]	0.49	0.60	0.48	0.48	–
Σ[Zn–A][e]	0.36	0.32	0.52	0.29	–

[a] $\log K$ (ZnBH + BH) = 14.28; $\log K$ (ZnB + BH) = 13.81.
[b] $\log K$ (ZnB + B) = 4.77.
[c] $\log K$ (ZnA + A) = 4.72 (mal); 6.31 (dhp); 4.33 (pic); 3.96 (6-Me-pic); 6.52 (dipic).
[d] Conditional stability constants at pH 7.4.
[e] Summed molar fractions at pH 7.4; 1:2:2 Zn(II): ligand A: ligand B ratio, $c_{Zn(II)} = 2$ mM.
[f] $\log K$ (ZnB + B) = 2.52.

The $\log K$ values (see rows 6–9 in Table 3) in the case of GSH related to the coordination of $[BH]^{2-}$ to [ZnA] or [ZnA$_2$] cores show similarity to the binding of $[BH]^{2-}$ in the bis parent complexes of GSH, suggest a similar coordination mode of $[BH]^{2-}$, namely the monodentate thiolate

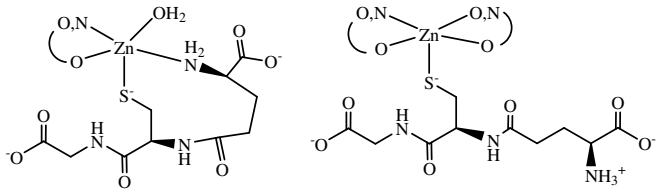

Scheme 2. Proposed structures for the ternary complexes [ZnA(GSH)] and [ZnA$_2$(GSH)H] of the bidentate ligands A.

binding of the ligand. A proposed structure for [ZnA$_2$BH] in the case of bidentate ligands A can be seen in Scheme 2.

The derived constants for the process [ZnA] + B ⇌ [ZnAB] are always much higher than the related constant for the equilibrium [ZnB]+B ⇌ [ZnB$_2$]. The stronger binding of GSH in the ternary complex can be interpreted in the different (S^-, NH_2(Glu)) coordination as compared with the monodentate (S^-) coordination of the second GSH molecule in the bis parent complex, what makes formation of the mixed-ligand complexes more favoured. Similarly, a favoured ternary complex formation can be observed with ATP considering the $\log K$ (ZnA + B) values (see row 16 in Table 3), which are higher by at least one $\log K$ unit than the corresponding $\log K$ (ZnB + B) in all cases. The stronger binding of ATP molecule to a [ZnA] core compared to [ZnB] can be interpreted by sterically and electrostatically more favoured coordination of the ligand in the ternary species. Since the $\log K$ (ZnB + A) values (see row 18 in Table 3) are always similar or even smaller than the relevant $\log K$(ZnA + A) constants, it can be concluded that the favourable binding of ligands B to zinc(II) in the mixed-ligand complexes as compared to the binary complexes is the driving force of their formation.

The stability constants of the ternary complexes studied can not be compared directly, due to the different protonation processes of the carrier ligands, therefore the pH

dependence of the conditional stability constants of the mixed-ligand complexes [ZnABH] and [ZnAB] for physiological pH were calculated and they are listed in Table 3 (see the log $\log\beta^*$ values in Table 3). As in the case of the parent complexes of the carrier ligands an almost similar tendency in the stability order can be found with the ternary complexes showing the outstandingly favoured formation of the dipic complex. The conditional stability constant of pic also exceed those of 6-Me-pic, dhp and mal. Furthermore, the values suggest similar coordination modes of ligands A in both the parent and the mixed-ligand complexes.

As an illustration, the extent of formation of the mixed-ligand complexes and the parent complexes are compared in the summed concentration distribution curves (the sums of the zinc(II) fractions bound in the binary complexes with ligand A or B and those bound in the ternary complexes with ligands A and B as a function of pH) in Fig. 3 for the ternary systems of 6-Me-pic and dipic in the case of GSH and for 6-Me-pic with ATP. The speciation curves demonstrate that mixed-ligand complexes are present in high proportion at physiological pH in the case of 6-Me-pic systems, while dipic forms ternary species with GSH only in the more basic pH range. On the other hand, the lack of ternary complex formation with ATP in the measured pH range also demonstrates the importance of the strong zinc(II)–thiolate binding of GSH which can better compete with the donor atoms of dipic for coordination to zinc(II).

The summed molar ratios of species formed with ligands A (Σ[Zn–A]) and those of ternary complexes (Σ[Zn–A–B]) were calculated and listed in Table 3 (rows 13,14,20 and 21) at physiological pH for all insulin–mimetic complexes studied in the present work. Data show an enhanced ternary complex formation with all ligands. The tridentate dipic, and among the bidentate carrier ligands pic are able to remain mostly in the original form of the insulin–mimetic complex.

In the case of zinc(II)–mal–GSH system UV and CD measurements were performed as a function of pH in order to study the extent of ternary complex formation. Since both mal and GSH ligands absorb at wavelength lower than 270 nm, UV spectra were analysed in the range of 270–370 nm, where exclusively mal and zinc(II) complexes of mal do. (ε [HA] = 8600 $M^{-1}cm^{-1}$ (274 nm); ε $[A]^-$ = 7508 $M^{-1}\,cm^{-1}$ (320 nm); ε $[ZnA]^+ = 9104$ $M^{-1}cm^{-1}$ (312 nm); ε $[ZnA_2] = 12{,}770$ $M^{-1}cm^{-1}$ (308 nm)) values were determined from independent measurements of the ligand and the Zn(II)–mal binary systems.) These spectroscopic measurements provide only indirect evidences for ternary complex formation. Namely, the tendency of changes in UV absorbances as a function of pH in the ternary system corresponds to the expectations based on the concentration distribution of mal as compared to the zinc(II)–mal system. However, CD spectra of the ternary system show measurable differences from those of zinc(II)–GSH above pH 9 in the range of development of the characteristic band with negative Cotton-effect due to complex $[ZnB_2H_{-2}]^{6-}$ (see Section 3.1.2), since its formation is suppressed by the formation of the mixed-ligand complexes.

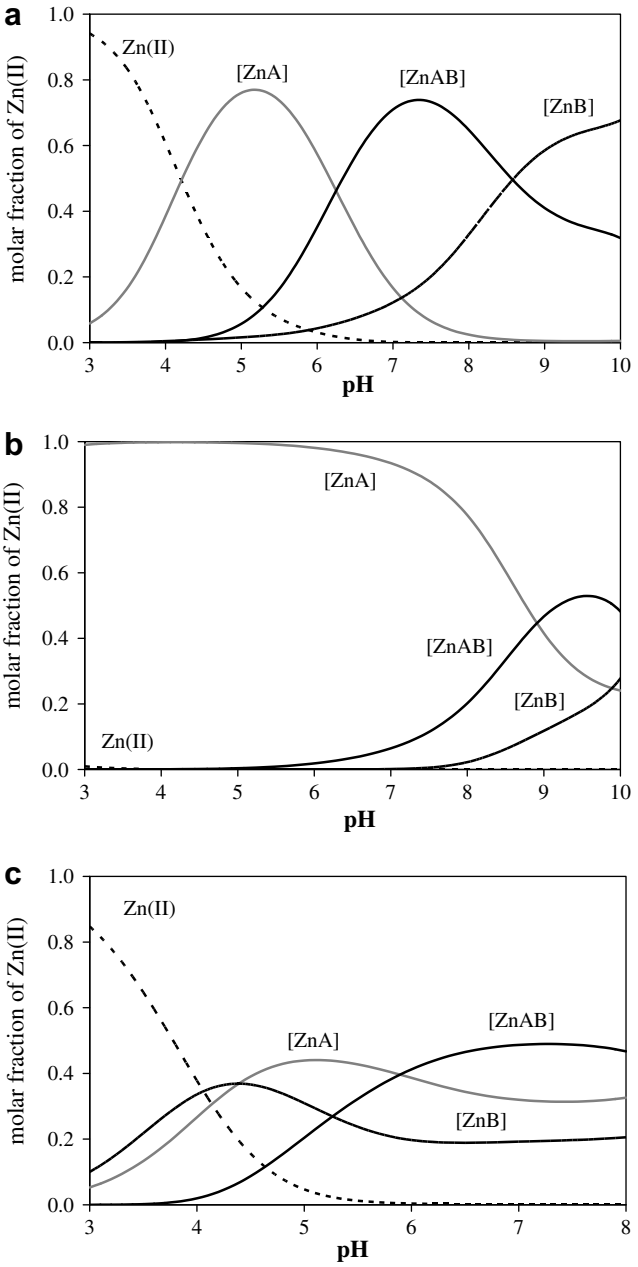

Fig. 3. Summed concentration distribution curves for complexes formed in the Zn(II)–6-Me-pic–GSH (a) Zn(II)–dipic–GSH (b) and Zn(II)–6-Me-pic–ATP (c) systems at 1:2:2 ratio, $c_{Zn(II)} = 2$ mM.

3.3. ESI-MS characteristics of the binary and ternary systems

ESI-MS measurements were also carried out to confirm the formation of mixed-ligand complexes with GSH. ESI-MS is increasingly used to study ternary systems because the interpretation of spectra is relatively easy [39], although

some limitations in studying of solution equilibria must be taken into account: (i) ESI-MS gives only a qualitative picture of the system studied, (ii) only the metal–ligand stoichiometries could be determined, the original proton content of the complexes in solution can not be evaluated, because proton transfer reactions are activated by the ESI method and furthermore the formation of single charged species is highly favoured in these conditions.

The best spectra for the solutions containing zinc(II), the carrier ligand (A) and GSH (B) were obtained in positive ion mode. Identification of the detected ions was done on the basis of m/z ratios, isotopic pattern and MS^n experiments. The main signals detected at pH 7 are reported in Table 4 together with the corresponding species (at the same metal-ligand ratios) found by potentiometry.

The base peak (100%) in most of the spectra is that of the fully protonated GSH ($[GSH + H]^+$) at m/z 308. The sodium adduct of GSH $[GSH + Na]^+$ at m/z 330 and in the binary GSH system the proton bound cluster $[(GSH)_2 + H]^+$ at m/z 615 could also be detected. The carrier ligand molecule A is detected as $[H_2A]^+$, except dipic, where the signal of the free ligand is missing from the spectrum. This could be a consequence of the different charge of the species in solution: dipic is double negatively charged at pH 7 with respect to the other ligands which are simply charged or neutral. Thus, to be detectable in positive ion mode, dipic should take up three protons, which is not favoured at neutral pH since the two carboxylic groups of dipic have very low basicity (see Table 1). The signals of the zinc(II) complexes were assigned on the basis of m/z ratios and isotopic pattern. The peak at m/z 370 was attributed to the binary 1:1 complex of GSH, $[ZnBH_2]^+$, which corresponds to the species $[ZnB]^-$ found potentiometrically. For the binary complexes formed with the carrier ligands 1:1 and 1:2 metal–ligand stoichiometries were observed, in agreement with potentiometric data. The 1:1 species were detected as solvent adducts giving rise to a series of signals depending on the nature of the attached solvent molecules (water or ACN). The binary complexes have been studied and characterised in detail in separate papers [5, A. Lakatos, R. Seraglia, P. Traldi, T. Kiss, manuscript in preparation]. Formation of solvent adducts was observed also in the case of oxovanadium(IV) complexes of the same ligand molecules [A. Lakatos, R. Seraglia, P. Traldi, T. Kiss, manuscript in preparation]. Besides the peaks of binary complexes a signal assigned to the ternary complex of 1:1:1 metal – carrier ligand – GSH stoichiometry was detected as $[ZnABH_3]^+$ for mal, dhp, pic and 6-Me-pic and as $[ZnABH_4]^+$ for dipic, at m/z values listed in Table 4. A typical mass spectra for the zinc(II)–mal–GSH system is depicted in Fig. 4. The insets of this figure show that the measured isotopic distribution pattern of the ternary complex $[ZnABH_3]^+$ at m/z 496 (inset A) corresponds well with that calculated one for the same composition $[C_{16}H_{22}N_3O_9SZn]^+$ (inset B). This proves unambiguously the formation of the ternary complexes.

Table 4
Signals identified in the ESI-MS spectra of solutions containing Zn(II), carrier ligand (A) and GSH (B) and the corresponding species found by potentiometry

System Zn(II)–A–B	Peaks (m/z)	Relative abundance (%)	Stoichiometries	Corresponding species found by potentiometry
A = **mal**	127	39	$[H_2A]^+$	[HA], $[A]^-$
B = GSH	207	31	$[ZnA \cdot H_2O]^+$	$[ZnA]^+$
	230	42	$[ZnA \cdot ACN]^+$	
	308	100	$[H_4B]^+$	[H_2B], $[HB]^{2-}$
	330	25	$[NaH_3B]^+$	
	315	35	$[ZnA_2H]^+$	$[ZnA_2]$
	370	17	$[ZnBH_2]^+$	$[ZnB]^-$
	496	16	$[ZnABH_3]^+$	$[ZnAB]^{2-}$
A = **dhp**	140	100	$[H_2A]^+$	[HA]
B = GSH	243	8	$[ZnA \cdot ACN]^+$	$[ZnA]^+$
	308	25	$[H_4B]^+$	$[H_2B]^-$, $[HB]^{2-}$
	341	16	$[ZnA_2H]^+$	$[ZnA_2]$
	370	10	$[ZnBH_2]^+$	$[ZnB]^-$
	509	12	$[ZnABH_3]^+$	$[ZnABH]^-$
A = **pic**	124	15	$[H_2A]^+$	$[A]^-$
B = GSH	227	19	$[ZnA \cdot ACN]^+$	$[ZnA]^+$
	308	100	$[H_4B]^+$	$[H_2B]^-$, $[HB]^{2-}$
	330	13	$[NaH_3B]^+$	
	309	68	$[ZnA_2H]^+$	$[ZnA_2]$
	370	9	$[ZnBH_2]^+$	$[ZnB]^-$
	493	10	$[ZnABH_3]^+$	$[ZnAB]^{2-}$
A = **6-Me-pic**	138	52	$[H_2A]^+$	[HA], $[A]^-$
B = GSH	218	11	$[ZnA \cdot H_2O]^+$	$[ZnA]^+$
	241	5	$[ZnA \cdot ACN]^+$	
	308	100	$[H_4B]^+$	$[H_2B]^-$, $[HB]^{2-}$
	330	56	$[NaH_3B]^+$	
	337	34	$[ZnA_2H]^+$	$[ZnA_2]$
	370	25	$[ZnBH_2]^+$	$[ZnB]^-$
	507	15	$[ZnABH_3]^+$	$[ZnAB]^{2-}$
A = **dipic**	308	100	$[H_4B]^+$	$[H_2B]^-$, $[HB]^{2-}$
B = GSH	330	38	$[NaH_3B]^+$	
	397	27	$[ZnA_2H_3]^+$	$[ZnA_2]^{2-}$
	537	8	$[ZnABH_4]^+$	$[ZnAB]^{3-}$

Molecular masses of the neutral ligand molecules: 126 for mal, 139 for dhp, 123 for pic, 137 for 6-Me-pic, 139 for dipic and 307 for GSH.

Detailed characterization of these ternary complexes has been made by collisionally induced fragmentation experiments (MS^n). In the case of mal, pic, 6-Me-pic and dipic fragmentation of the ternary complex results in the appearance of a signal at m/z 370 which was attributed to the zinc(II) complex $[ZnBH_2]^+$. This is consistent with the loss of a neutral carrier ligand molecule (mal, pic, 6-Me-pic and dipic), expulsion of 126, 123, 137 and 307 Da, respectively. Fragmentation of the $[ZnABH_3]^+$ complex of dhp at m/z 509 is slightly different: it gives two fragments at m/z 491 and 370, the first one being more abundant. The ionic species at m/z 491 is due to the loss of a water molecule formed from one of the coordinated oxygens of the fragmented dhp, whereas the fragment at m/z 370 is again the result of the expulsion of the carrier ligand (139 Da). These results indicate that zinc(II) is more strongly bound to GSH than to the carrier ligands under ESI conditions.

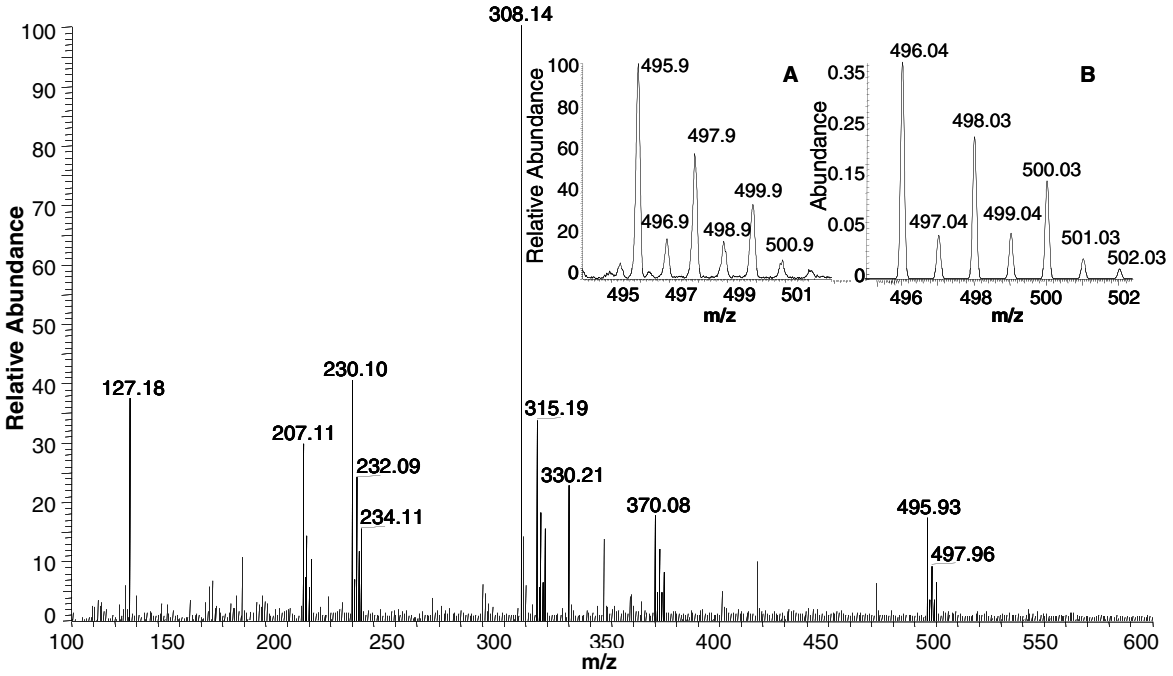

Fig. 4. ESI-MS spectra recorded in the Zn(II)–mal–GSH system at 1:2:2 ratio and pH 7. Inset: (A) zoom scan spectrum of the peak at *m/z* 496 attributed to the ternary complex $[ZnABH_3]^+$ and (B) calculated isotopic distribution pattern for the composition $[C_{16}H_{22}N_3O_9SZn]^+$.

Breakdown curves (relative intensities of the precursor ion and its fragments *vs.* rf voltages applied in the collision experiment) of the complexes $[ZnABH_3]^+$ (data not shown) reveal that the crossing point between the decreasing abundance of the precursor ion $[ZnABH_3]^+$ and the increasing abundance of the fragment ion $[ZnBH_2]^+$ is at 0.783V for mal, 0.911 for pic, 0.948 for 6-Me-pic and at 0.994 for dipic. This indicates that disruption of the bonds formed through the coordination of oxygen donor groups is more favoured energetically, than disruption of the bonds involving nitrogen, which means a stronger coordination of the latter, in accordance with the nitrophilic nature of zinc(II). It seems that there is a correlation between the energy necessary for the cleavage of bonds between ligand A and zinc(II) and the conditional stability constants of the ternary complexes in solution (see Table 3), i.e. the higher the rf. voltage corresponding to the crossing point where the concentration of the precursor ion is equal to the concentration of the fragment, the higher the stability constant of the ternary complexes.

Fragmentation of the zinc(II)–GSH complex $[ZnBH_2]^+$ at *m/z* 370 (either as the original species present in the spectra or as the fragment ion of the ternary complexes) occurs with loss of a glycine molecule affording an ionic species at *m/z* 295. This represents the main fragmentation pathway of the precursor ion. Other decompositions take place with the loss of a water molecule most probably from the carboxylic group of glycine and with the expulsion of a neutral molecule with mass of 103 Da – a formamide derivative of glycine (see Scheme 3) – leading to the formation of the ionic species at *m/z* 267. The main fragment at *m/z* 295

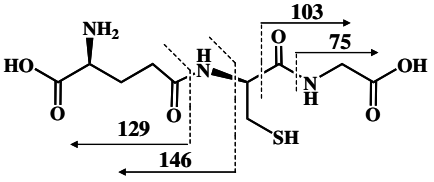

Scheme 3. Characteristic fragments of GSH detected during MS^n experiments.

loses a CO molecule from the cysteinyl moiety in the MS^3 experiment with the formation of the species at *m/z* 267. This fragment decomposes in the next step by expulsion of a water molecule from the carboxylic group of glutamic acid moiety resulting in the ionic species at *m/z* 249. In the next fragmentation step this ion gives the ion at *m/z* 221 consistent with the loss of a CO molecule from the side-chain carboxylic group. Since the neutral fragments lost do not contain sulphur and the zinc(II) remains in the positively charged ionic forms the thiolate group is most probable remains coordinated to zinc(II).

For a comparison of the fragmentation of the zinc(II)-bound and free GSH the fragmentation of $[H_4B]^+$ ion at *m/z* 308 was also carried out. Three fragment ions were observed in the MS^2 experiments at *m/z* 179, 233 and 162. The assignment of these fragments and neutral losses has been made on the basis of literature data [40]. The most abundant fragment ion is that leading the signal at *m/z* 179 which is formed through the neutral loss of a glutamic acid residue with a mass of 129 Da (Scheme 3). The appearance of the fragment ion at *m/z* 233 is consistent with the loss of

a glycine, whereas the fragment at *m/z* 162 is the result of the expulsion of glutamine (Scheme 3). Further decomposition of the main fragment at *m/z* 179 occurs with consecutive losses of one ammonia from the amino group of the cysteinyl moiety, one molecule of water, CO and methanimine ($H_2C{=}NH$) from the glycinyl moiety, leading finally to the ionic species at *m/z* 88 with the formulae $C_3H_4O_3S$. These experiments show that fragmentation of GSH starts parallel at both ends of the molecule (Glu and Gly), while in the zinc(II) complex of GSH only the carboxylic end (Gly) is affected. This may suggest that the glutamate residue is "fixed" in the zinc(II)–GSH complex $[ZnBH_2]^+$ most probably due to the coordination of the terminal amino group in accordance with the binding mode in [ZnAB] complexes suggested by the pH-potentiometric data.

3.4. Biological activity of the zinc(II) complexes

In order to assess the potential applicability of these compounds to decrease cell glucose level toxicity and EZ4U tests were carried out.

Toxicity tests were performed on Mono Mac human cells by incubation with solutions of the zinc(II) complexes for 48 h at different concentrations: 1, 10, 100 and 1000 μM. Incubation was followed by the addition of PI solution. In this dye exclusion assay live and dead cells can be differentiated with the use of PI dye. By the losing of membrane integrity the dye penetrates the dead cells and emits a red fluorescence after binding to cellular DNA or double stranded RNA. Results are represented in Fig. 5. Solid base line shows the toxicity measured for the buffer solution at 0 μM concentration of zinc(II). At zinc(II) concentration below 100 μM complexes were practically non-toxic. A slight increase in toxicity could be measured with increasing concentration of the pic and dipic complexes and only the zinc(II)–maltol solution showed considerable toxic effect at the highest, 1000 μM, concentration. When the results of the toxicity tests are compared with those of the corresponding vanadium compounds [7], it becomes clear that in accordance with the expectations the zinc(II) complexes are considerably less toxic.

The insulin–mimetic potency of metal complexes is usually expressed in terms of their blood glucose level lowering ability, but information about the effect of the complexes in simplified manners can also be measured on cells *in vitro*. In the present study the glucose intake was assessed by a test based on an EZ4U assay. This assay depends on the production of formazan derivatives, which requires functional mitochondria. There might be a relationship between the mitochondrial dehydrogenase activity and the extent of glucose intake into the cells, and hence the effect of the zinc(II) complexes studied can be compared to that of insulin [7]. Results show a minimal increase in the metabolic activity in the case of pic and dipic up to 10 μM concentration, while mal seems to be almost ineffective on Mono Mac cells in the studied concentration range as it can be seen in Fig. 6a. With elevating the zinc(II) complex concentration higher than 100 μM the vitality of the cells tends to show a definite loss with pic and especially with mal, most probably due to the higher toxicity of these complexes at higher concentrations (see Fig. 5). On the contrary, dipic shows an increased mitochondrial dehydrogenase activity with increasing concentration, thanks to its less toxic effect on the studied Mono Mac cell line. In accordance with these

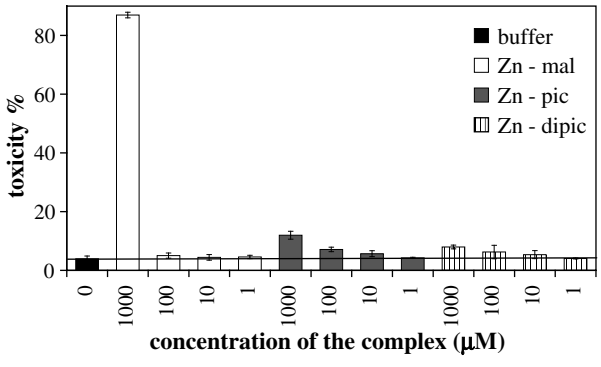

Fig. 5. *In vitro* IP toxicity assay of zinc(II) complexes at different concentrations ($c = 1$, 10, 100, 1000 μM) in the case of mal (white bars), pic (grey bars), dipic (stripe bars) and buffer (black bar) on Mono Mac cell lines.

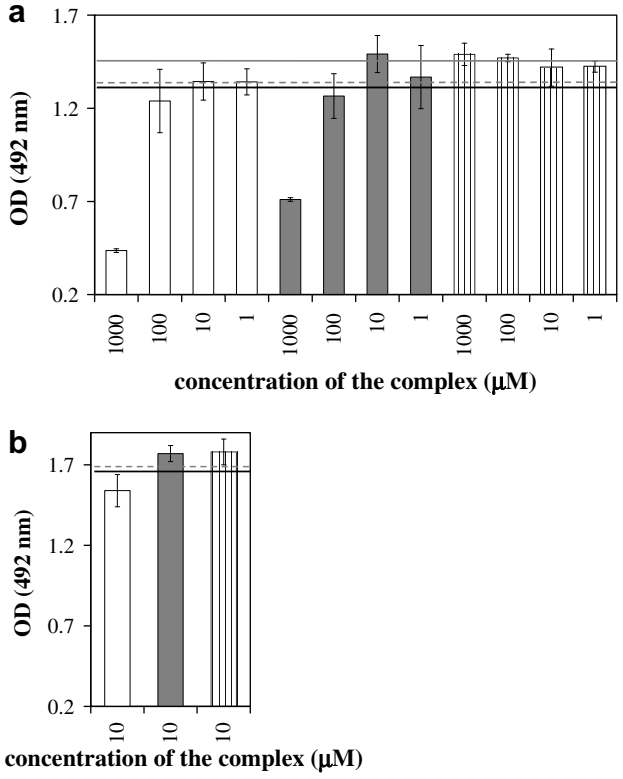

Fig. 6. *In vitro* EZ4U assay on Mono Mac (a) and on 3T3-L1 adipocyte (b) cell lines related on the glucose intake in the presence of zinc(II) complexes at different concentrations (mal: white bars, pic: grey bars, dipic: stripe bars) and for insulin at 0.75 (dashed grey line) and 1.5 μM concentrations (solid grey line) and for the control (solid black line).

results Sakurai et al. found similar insulin-like activity of the zinc(II) complexes of mal and pic based on the *in vitro* measurements of the inhibition of the free fatty acids release on isolated rat adipocytes (IC_{50} values) [3,16,18]. The insulin-like effect was tested on 3T3-L1 adipocyte cells too, at 10 μM complex concentration (see Fig. 6b). Zinc(II)-picolinato and zinc(II)-dipicolinato showed similar increased metabolic activity, but zinc(II)-maltolato somewhat lower activity as compared to the control. This cell line, however, was less sensitive to the biological assay and thus the results are less reliable.

Although these test results do not relate directly to an increased glucose uptake of the cells, the agreement with the results of the free fatty acid release test of Sakurai may suggest that the test can be used as a draft assessment in such studies before direct glucose uptake measurements by radiolabelled ^{3}H-glucose.

4. Conclusions

Several bidentate (O,O) and (O,N) donor ligands were found to form relatively high stability coordinatively unsaturated neutral bis complexes with zinc(II), at the same time dipicolinate, this tridentate pic derivative forms a coordinatively saturated exceptionally stable charged bis complex with this metal ion. Biological studies showed that the effect of the studied zinc(II) complexes at 1–10 μM concentrations on the mitochondrial dehydrogenase activity, as an indirect assessment of glucose intake, falls into the range of the action of 0.75–1.5 μM insulin, but no significant differences could be measured between the studied zinc(II) complexes on Mono Mac cell line, whereas pic and mal represent somewhat ascendant metabolic activity upon increasing complex concentrations (especially at 1 mM). Most probably the weakened effect is due to the sensitivity of these cells to the toxicity of the complexes of mal and pic.

The amount of zinc(II) bound by the high molecular mass proteins (like metallothionein and zinc(II) specific chaperons) of the cell are less mobile, while the zinc(II) bound to the low molecular mass binders, which are much more mobile, are more easily exchangeable. Accordingly, speciation of this fraction is especially important. When studying the interactions of the zinc(II) complexes with GSH and ATP, the critical high concentration low molecular mass zinc(II) binder constituents of cytosol, enhanced ternary complex formation was found in the physiological pH range with all binary zinc(II) carrier complexes. At the same time that was hindered with the tridentate dipicolinate and occurred only in the basic pH range. Due to the presence of the same binding oligophosphate moiety similarly favoured ternary complex formation can be expected with other nucleotides and most of the organophosphates.

The stability constants calculated for the ternary complexes of GSH and ATP formed with ligands A studied may allow us a rough estimation of the fate of the insulin–mimetic complex when (if any) reaches the cytosol. It is very likely however, that distribution of zinc(II), GSH, ATP and the carrier ligand is also under kinetic control. Unfortunately, there is no data available related to the enhanced zinc(II) concentration in the cell followed by the administration of the insulin–mimetic complex and to the local concentration of GSH and ATP. Considering the IC_{50} values of the insulin–mimetic complexes [3,16,18], which represent the concentrations where the inhibition of the free fatty acid release stimulated by epinephrine in adipocytes is 50%, which fall into the millimolar range and the concentration of the cell constituents in question in the cytosol is up to 20 mM [9,10], As an illustration of the extent of ternary complex formation, speciation curves were calculated in the case of 6-Me-pic at physiological pH at different concentrations of GSH or ATP and found that formation of the ternary complexes are significant in the 0.01–10 mM concentration range with both GSH and ATP. When the effects of both cellular components are considered together the more pronounced role of GSH in zinc(II) binding is revealed; *ca.* 65% of the metal ion is bound in binary or ternary complexes of GSH and only the rest to the nucleotide (see Fig. 7).

Furthermore, the turnover of ATP is very high in comparison to GSH. Accordingly, in the cell, ternary complexes may occur as new species with GSH. At the same time, ternary complex formations with ATP may be considered only as ways of their interference into the biological effects of the nucleotide.

No direct relationship between the biological results (neither the EZ4U test nor the IC_{50} values reported by Sakurai et al. [3,16,18]) and the extent of ternary complex formation with these important cell constituents was found. As was discussed in the Introduction the biological effect of Zn(II) is assumed to be connected with its interference with numerous phosphorylation/dephosphorylation steps of the glucose metabolic reaction cascade. Accordingly, a relationship between the biological activity and the extent of ternary complex formation of the Zn(II) complex with ATP was expected. In this behaviour there is a big difference between the tridentate dipicolinate and the

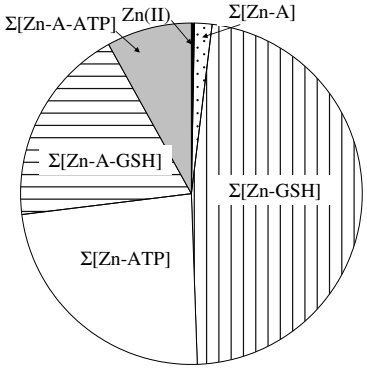

Fig. 7. Summed concentration distribution diagram for complexes formed in a Zn(II)–6-Me-pic–GSH–ATP hypothetic systems at physiological pH, $c_{Zn(II)} = 0.10$ mM, $c_{6\text{-Me-pic}} = 0.2$ mM, $c_{GSH} = 1$ mM, $c_{ATP} = 1$ mM.

rest of the bidentate ligands. However, as shown in Fig. 6, the difference between the biological effects of the various zinc(II) complexes studied is small similarly to the IC_{50} values (see Experimental), which does not allow a search for reliable correspondence with the thermodynamic equilibrium. It seems probable that other factors such as membrane transport properties of the antidiabetic zinc(II) complexes or the time course of their reactions can also affect the biological activity more significantly.

5. Abbreviations

6-Me-pic 6-methylpicolinic acid
ACN acetonitrile
ADP adenosine 5′-diphosphate
AMP adenosine 5′-monophosphate
ATP adenosine 5′-triphosphate
CD circular dichroism
dhp 3-hydroxy-1,2-dimethyl-pyridinone
dipic 2,6-dipicolinic acid
ESI-MS electrospray ionization mass spectrometry
FCS fetal calf serum
GSH γ-L-glutamyl-L-cysteinyl-glycine, L-glutathione reduced
GSSG oxidised L-glutathione
l path length
mal maltol
MLCT metal to ligand charge transfer
PBS phosphate buffered saline solution
PI propidium iodide
pic 2-picolinic acid

Acknowledgments

The authors thank Prof. Éva Monostori and Dr. Vilmos Tubak for the biological measurements and the help in the interpretation of the results. This work has been supported by the Hungarian Research Foundation OTKA NI61786, T049417 and PD050011. A.L. gratefully acknowledges the financial support of the Hungarian Scholarship Broad through the award of an Eötvös research fellowship.

References

[1] L. Coulston, P. Dandona, Diabetes 29 (1980) 665–667.
[2] H. Sakurai, A. Katoh, Y. Yoshikawa, Bull. Chem. Soc. Jpn. 79 (2006) 1645–1664.
[3] J. Fugono, K. Fujimoto, H. Yasui, K. Kawabe, Y. Yoshikawa, Y. Kojima, H. Sakurai, Drug Metabol. Pharmacokin. 17 (2002) 340–347.
[4] Y. Adachi, J. Yoshida, Y. Kodera, A. Kato, Y. Yoshikawa, Y. Kojima, H. Sakurai, J. Biol. Inorg. Chem. 9 (2004) 885–893.
[5] T. Jakusch, K. Gajda-Schrantz, Y. Adachy, H. Sakurai, T. Kiss, L. Horváth, J. Inorg. Biochem. 100 (2006) 1521–1526.
[6] Y. Yoshikawa, Y. Adachi, H. Sakurai, Life Sci. 80 (2007) 759–766.
[7] D. Rehder, J. Costa Pessoa, C.F.G.C. Geraldes, M.M.C.A. Castro, T. Kabanos, T. Kiss, B. Meier, G. Micera, L. Pettersson, M. Rangel, A. Salifoglou, I. Turel, D. Wang, J. Biol. Inorg. Chem. 7 (2002) 384–396.
[8] Y. Yoshikawa, E. Ueda, Y. Kojima, H. Sakurai, Life Sci. 75 (2004) 741–751.
[9] G. Wu, Y. Fang, S. Yang, J.R. Lupton, N.D. Turner, J. Nutr. 134 (2004) 489–492.
[10] Á. Dörnyei, S. Marcao, J. Costa Pessoa, T. Jakusch, T. Kiss, Eur. J. Inorg. Chem. (2006) 3614–3621.
[11] H. Tapiero, K.D. Tew, Biomed. Pharmacotherapy 57 (2003) 399–411.
[12] D.L. Rabenstein, A.A. Isab, FEBS Lett. 121 (1980) 61–64.
[13] S.M. Sato, J.M. Frazier, A.M. Goldberg, J. Neurosci. 4 (1984) 1662–1670.
[14] A.E. Martell, R.M. Smith, Critical Stability Constants, Plenum Press, New York, 1989.
[15] J.E. Coleman, D.P. Giedroc, in: A. Sigel, H. Sigel (Eds.), Metal Ions in Biological Systems, Zinc-Binding Proteins Involved in Nucleic Acid Replication, vol. 25, Marcel Dekker, New York, 1989, p. 171.
[16] H. Sakurai, Y. Kojima, Y. Yoshikawa, K. Kawabe, H. Yasui, Coord. Chem. Rev. 226 (2002) 187–198.
[17] Y. Yoshikawa, E. Ueda, H. Miyake, H. Sakurai, Y. Kojima, Biochem. Biophys. Res. Comm. 281 (2001) 1190–1193.
[18] Y. Yoshikawa, E. Ueda, K. Kawabe, H. Miyake, T. Takino, H. Sakurai, Y. Kojima, J. Biol. Inorg. Chem. 7 (2002) 68–73.
[19] É. A. Enyedy, L. Horváth, K. Gajda-Schrantz, G. Galbács, T. Kiss, J. Inorg. Biochem. 100 (2006) 1936–1945.
[20] G. Gran, Acta Chem. Scand. 4 (1950) 559–577.
[21] H.M. Irving, M.G. Miles, L.D. Pettit, Anal. Chim. Acta 38 (1967) 475–488.
[22] L. Zékány, I. Nagypál, in: D.L. Leggett (Ed.), Computational Methods for the Determination of Stability Constants, Plenum Press, New York, 1985.
[23] N. Yasumatsu, Y. Yoshikawa, Y. Adachi, H. Sakurai, Bioorg. Med. Chem. 15 (2007) 4917–4922.
[24] Y. Zhang, X. Yang, K. Wang, D.C. Crans, J. Inorg. Biochem. 100 (2006) 80–87.
[25] T. Jakusch, W. Jin, L. Yang, T. Kiss, D.C. Crans, J. Inorg. Biochem. 95 (2003) 1–13.
[26] Z. Vargová, V. Zeleòák, I. Ćısaøová, K. Györyová, Thermochim. Acta 423 (2004) 149–157.
[27] L.C. Nathan, D.C. Zapien, A.M. Mooring, C.A. Doyle, J.A. Brown, Polyhedron 8 (1989) 745–748.
[28] A. Krezel, J. Wojcik, M. Maciejczyk, W. Bal, Chem. Commun. (2003) 704–705.
[29] A. Krezel, W. Bal, Bioinorg. Chem. Appl. 2 (2004) 293–305.
[30] T. Kiss, in: K. Burger (Ed.), Biocoordination Chemistry, Ellis Horwood, London, 1990, pp. 171–172.
[31] B.J. Fuhr, D.L. Rabenstein, J. Am. Chem. Soc. 95 (1973) 6944–6950.
[32] M. Vasak, J.H. Kagi, H.A. Hill, Biochem. 20 (1981) 2852–2856.
[33] A. Armas, V. Sonois, E. Mothes, H. Mazarguil, P. Faller, J. Inorg. Biochem. 100 (2006) 1672–1678.
[34] R. Tribolet, H. Sigel, Eur. J. Biochem. 170 (1988) 617–626.
[35] H. Sigel, K.H. Scheller, R.M. Milburn, Inorg. Chem. 23 (1984) 1933–1938.
[36] H. Sigel, Eur. J. Biochem. 165 (1987) 65–72.
[37] P. Gockel, R. Vogler, M. Gelinsky, A. Meissner, H. Albrich, H. Vahrenkamp, Inorg. Chim. Acta 323 (2001) 16–22.
[38] M. Rombach, M. Gelinsky, H. Vahrenkamp, Inorg. Chim. Acta 334 (2002) 25–33.
[39] V.B. Di Marco, G.G. Bombi, Mass Spectr. Rev. 25 (2006) 347–379.
[40] N. Burford, M.D. Eelman, K. Groom, J. Inorg. Biochem. 99 (2005) 1992–1997.